ARCHIVE OF MECHANICAL ENGINEERING

DOI: 10.24425/ame.2025.153732 2025, Vol. 72, No. 1, pp. 57–83

Sami SOUISSI [1], Mohamed BOUKATTAYA [2], Chiheb ZAOUI[1]

Adaptive dual-loop trajectory tracking control of marine surface vehicles in the presence of kinematic and dynamic disturbances

Received 5 October 2024, **Revised** 13 December 2024, **Accepted** 8 January 2025, **Published online** 23 January 2025

Keywords: Marine Surface Vehicle (MSV), double-loop control, adaptive control, ocean current estimation, marine disturbance

This paper introduces a dual-loop adaptive trajectory tracking control system for Marine Surface Vehicles (MSVs) that addresses both kinematic and dynamic disturbances. The approach begins with an outer-loop backstepping control strategy, which generates velocity commands at the kinematic level to ensure accurate tracking of the MSV's position and heading. An adaptive estimator is integrated to assess unknown ocean current velocities, allowing for effective compensation of their impact. The inner-loop control employs linear parameterization to produce torque commands at the dynamic level, ensuring alignment between the actual and commanded velocity states. Two adaptive tuning laws are proposed: one for estimating challenging hydrodynamic parameters and another for compensating external marine disturbances. The double-loop control significantly mitigates the effects of both kinematic and dynamic disturbances, enhancing the precision of MSV tracking and overall performance. Stability of the closed-loop system is established using Lyapunov theory, and the adaptation laws for the system's unknown parameters are derived. Numerical simulations demonstrate the efficacy of the proposed control strategy.

✉ Mohamed BOUKATTAYA, email: mohamed.boukattaya@gmail.com

[1]Marine Technology and Naval Systems Research Laboratory, Naval Academy, Tunisia. Emails: sami.souissi76@gmail.com, chiheb.zaoui@gmail.com

[2]Laboratory of Sciences and Techniques of Automatic Control and Computer Engineering (LabSTA), National School of Engineering of Sfax (ENIS), University of Sfax, Tunisia.

1. Introduction

Marine surface vehicles (MSVs) play a vital role in numerous ocean-based applications, including resource exploration, offshore surveillance, and oceanographic research [1–3]. However, achieving effective control of MSVs in complex marine environments remains challenging due to external disturbances like ocean currents, winds, and waves, along with parametric uncertainties. As a result, designing adaptive and robust control systems for these vehicles has become a significant research focus.

To tackle these complexities, researchers have explored a variety of advanced control techniques for MSVs, including machine learning-based methods and their derivatives, such as fuzzy control [4–6], neural networks (NN) [7–9], reinforcement learning (RL) [10–12], and event-triggered control [13–15]. Each approach offers unique benefits to improve adaptability and enhance real-time disturbance handling capabilities. Fuzzy control, for example, is known for its adaptability through rule-based systems, effectively addressing unpredictable factors like unknown ocean currents [4]. Similarly, neural network-based methods employ adaptive structures to manage uncertainties and meet time-varying constraints [7]. Deep learning (DL) and reinforcement learning (RL) techniques have recently gained traction for their data-driven adaptability and decision-making capacity in real-time, as seen in recent surveys highlighting advancements in DL and RL for MSV control [10]. Event-triggered control has also been explored to increase efficiency by updating controls only as necessary, thus minimizing computational load. For instance, event-triggered trajectory tracking with state and input quantization has been investigated [13], while other methods focus on simultaneous tracking and stabilization with limited inputs [14, 15]. These approaches contribute to improving MSV control efficiency by selectively activating updates based on system requirements.

Despite the potential of these machine learning-based techniques, they come with limitations such as the need for extensive datasets and high computational demands. In contrast, sliding mode control (SMC) offers a simpler and more robust alternative that effectively handles disturbances and uncertainties without requiring large datasets. Advanced SMC variants, such as finite-time [16–20], fixed-time [21–24], and predefined-time SMC [25–27], enhance performance by ensuring convergence within specific time constraints. Finite-time SMC, for instance, has been successfully applied to MSVs for heading tracking [16], path-following [17], and fault tolerance [19, 20], achieving robust performance by guaranteeing timely convergence. Fixed-time SMC provides convergence guarantees regardless of initial conditions, which is particularly valuable in marine environments [21]. Predefined-time SMC further improves on this by specifying an exact convergence time, making it suitable for time-sensitive applications [25–27]. While traditional SMC is effective, it has drawbacks, such as the "chattering" effect, characterized by high-frequency oscillations around the sliding surface, which can degrade control precision and lead to mechanical or electronic wear.

Furthermore, much existing MSV control research employs single-loop systems focused on position and orientation stabilization in the earth-fixed frame. This approach, however, overlooks the fast-changing velocity variables in the body-fixed frame, limiting adaptability.

To address this limitation, a double-loop control structure, consisting of an outer loop for high-level trajectory planning and an inner loop for detailed velocity control, offers improved modularity and adaptability. While double-loop control is commonly used in mobile robot systems, it has not been widely adopted in MSVs applications. A notable technique to address parameter uncertainty at the dynamic level is parametric separation, which has been extensively employed in the literature for MSVs, especially under environmental uncertainties and operational constraints [28–38]. For example, recent studies have introduced self-triggered adaptive neural control frameworks to mitigate measurement sensitivity issues under deception attacks [36] and developed distributed optimal control with event-based mechanisms to improve coordination among multiple vehicles [37]. Additionally, research has proposed intermittent anti-competition communication mechanisms to support robust formation maneuvers in constrained communication environments [38]. Building on these foundations, this study presents a robust double-loop control scheme for MSVs that integrates the parametric separation technique. A distinctive feature of our approach is the design of an inner control loop with two adaptive laws: one for handling unknown hydrodynamic parameters and another for countering rapidly changing disturbances. This dual-adaptive structure enables precise MSV velocity tracking, even under uncertain dynamics and external disturbances. Unlike prior studies that primarily address disturbances within the inner loop, our method manages both internal and external disturbances, such as those from ocean currents, within a unified control framework.The primary contributions of this study are as follows:

1. We introduce a novel double-loop control system for MSVs that enhances robustness and adaptability when facing complex disturbances, distinguishing our approach from existing studies [4–27].

2. To address external kinematic disturbances, our scheme incorporates an adaptive law to estimate and compensate for these disturbances, ensuring reliable navigation in challenging open-sea conditions [28–34].

3. The dual-adaptive approach in the inner control loop increases efficiency and resilience by generating precise input torque, even with unknown dynamic parameters and significant marine disturbances.

4. The double-loop structure allows the outer loop to manage slower dynamics while enabling the inner loop to respond quickly to faster dynamics, resulting in improved performance and resilience under demanding marine conditions.

This reminder is organized as follows: in Section 2, we present some preliminaries and a problem description of the MSV. Section 3 introduces the design analysis and main results of the proposed double-loop controller. The effective-

ness of the suggested controller is verified by numerical simulations in Section 4. Section 5 concludes the study.

2. Preliminaries and Problem Description

To accurately describe the motion of the MSV, it is crucial to establish two reference coordinate frames (Fig. 1). The first is the Earth-fixed frame, denoted as frame $\Re_E\,(O_E, X_E, Y_E, Z_E)$, with its origin at point O_E, where the O_EX_E – axis points to the north and the O_EY_E – axis points to the east. The second is the Body-reference frame, denoted as frame $\Re_B\,(O_B, X_B, Y_B, Z_B)$, with its origin at point O_B, where the O_BX_B – axis points forward to the bow, the O_BY_B – axis points toward starboard, and the O_BZ_B – axis points downward.

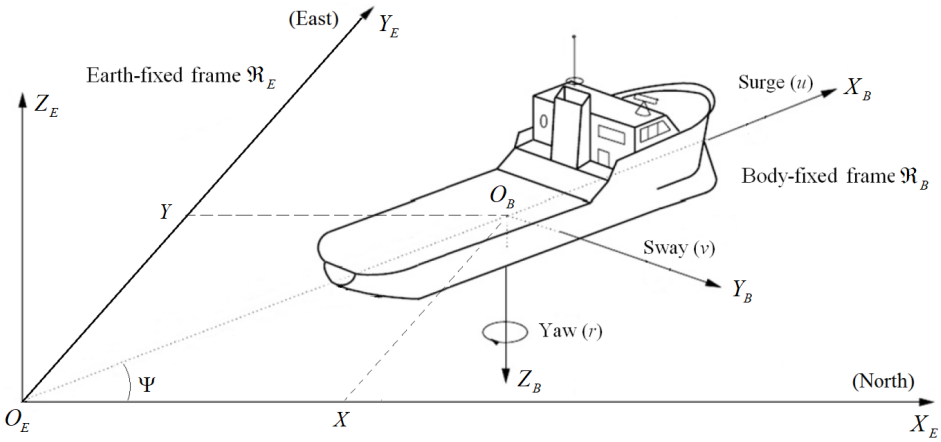

Fig. 1. The MSV frames and coordinate system

Using the previously mentioned frames, the system's posture describing the position and orientation of the MSV in the earth-fixed frame can be described as follows:

$$P(t) = \begin{bmatrix} X(t) & Y(t) & \Psi(t) \end{bmatrix}^T, \tag{1}$$

where X and Y represent the absolute position in the O_EX_E direction and O_EY_E direction respectively, and Ψ is the heading angle.

Furthermore, the system's velocity, which describes the velocities of the MSV in the body-fixed frame, can be described as follows:

$$\omega(t) = \begin{bmatrix} u(t) & v(t) & r(t) \end{bmatrix}^T, \tag{2}$$

where u and v denote the forward and transverse velocities in the O_BX_B and O_BY_B directions, often referred to as surge and sway velocities, and r represents the angular velocity typically known as yaw.

The kinematic model of the MSV is the mathematical relationship that describes the connection between the temporal derivative of its posture and the vehicle's speed. This model is expressed as:

$$\dot{P}(t) = \begin{bmatrix} \dot{X}(t) \\ \dot{Y}(t) \\ \dot{\Psi}(t) \end{bmatrix} = \begin{bmatrix} \cos\Psi & -\sin\Psi & 0 \\ \sin\Psi & \cos\Psi & 0 \\ 0 & 0 & 1 \end{bmatrix} \begin{bmatrix} u(t) \\ v(t) \\ r(t) \end{bmatrix} = R(\Psi)\,\omega(t), \tag{3}$$

where $R(\Psi)$ is the transformation matrix.

It's worth noting that in real marine applications, ocean currents can impact the motion of the marine vehicle. As a result, the expression of the kinematic model is modified as follows:

$$\dot{P}(t) = \begin{bmatrix} \dot{X}(t) \\ \dot{Y}(t) \\ \dot{\Psi}(t) \end{bmatrix} = \begin{bmatrix} \cos\Psi & -\sin\Psi & 0 \\ \sin\Psi & \cos\Psi & 0 \\ 0 & 0 & 1 \end{bmatrix} \begin{bmatrix} u(t) \\ v(t) \\ r(t) \end{bmatrix} + \begin{bmatrix} \rho_X(t) \\ \rho_Y(t) \\ 0 \end{bmatrix} = R(\Psi)\,\omega(t) + \rho(t), \tag{4}$$

where $\rho(t) = \begin{bmatrix} \rho_X(t) & \rho_Y(t) & 0 \end{bmatrix}^T$ represents the vector of ocean current velocity.

The dynamic model of the MSV is the mathematical relationship that explains how the applied force affects the vehicle's acceleration. This model can be described using the Euler-Lagrange formulation as follows:

$$M\dot{\omega}(t) + C(\omega)\omega(t) + D(\omega)\omega(t) = \Gamma(t) + \Delta(t), \tag{5}$$

where $M \in \Re^{3\times3}$ is the inertia matrix, $C(\omega) \in \Re^{3\times3}$ is the matrix representing Coriolis and centripetal forces, $D(\omega) \in \Re^{3\times3}$ is the damping matrix, $\Gamma(t) \in \Re^3$is the vector of control input and $\Delta(t) \in \Re^3$ is the vector of external disturbances. The specific expressions of the matrices M, $C(\omega)$, and $D(\omega)$ are given as follows:

$$M = \begin{bmatrix} m_{11} & 0 & 0 \\ 0 & m_{22} & m_{23} \\ 0 & m_{23} & m_{33} \end{bmatrix} = \begin{bmatrix} m - X_{\dot{u}} & 0 & 0 \\ 0 & m - Y_{\dot{v}} & mx_G - Y_{\dot{r}} \\ 0 & mx_G - Y_{\dot{r}} & I_Z - N_{\dot{r}} \end{bmatrix}, \tag{6}$$

$$\begin{aligned} C(\omega) &= \begin{bmatrix} 0 & 0 & c_{13}(v,r) \\ 0 & 0 & c_{23}(u) \\ -c_{13}(v,r) & -c_{23}(u) & 0 \end{bmatrix} \\ &= \begin{bmatrix} 0 & 0 & -m_{22}v - m_{23}r \\ 0 & 0 & m_{11}u \\ m_{22}v + m_{23}r & -m_{11}u & 0 \end{bmatrix}, \end{aligned} \tag{7}$$

$$D(\omega)=\begin{bmatrix} d_{11}(u) & 0 & 0 \\ 0 & d_{22}(v,r) & d_{23}(v,r) \\ 0 & d_{32}(v,r) & d_{33}(v,r) \end{bmatrix} = \begin{bmatrix} -X_u - X_{|u|u}|u| & 0 & 0 \\ 0 & -Y_v - Y_{v|v|}|v| - Y_{|r|v}|r| & -Y_r - Y_{|v|r}|v| - Y_{r|r|}|r| \\ 0 & -N_v - N_{|v|r}|v| - N_{r|r|}|r| & -N_r - N_{|v|r}|v| - N_{r|r|}|r| \end{bmatrix}. \tag{8}$$

In these equations, m is the mass of the MSV, I_z is its moment of inertia, and x_G is the center of gravity coordinate of the MSV. The hydrodynamic derivatives are denoted by X_*, Y_*, and N_*.

For the MSV system, the following properties hold.

Property 1 [33, 34] The inertia matrix M is characterized by being symmetric, positive-definite, and non-singular. Furthermore, it satisfies the following inequality.

$$m_{\min}\|\chi\|^2 \geqslant \chi^T M \chi \geqslant m_{\max}\|\chi\|^2 \quad \forall \chi \in \mathbb{R}^3, \tag{9}$$

where $m_{\min}$ and $m_{\max}$ are positive scalars.

Property 2 [33, 34] The matrix $\dot{M} - 2C(\omega)$ is skew symmetric and fulfills the subsequent equation:

$$\chi^T\Big(\dot{M} - 2C(\omega)\Big)\chi = 0 \quad \forall \chi, \omega \in \mathbb{R}^3. \tag{10}$$

Property 3 [33, 34] The dynamic model of the MSV (5) exhibits linear dependence on the parameters, which means it can be expressed as the product of two terms, as follows :

$$M\dot{\omega}(t) + C(\omega)\omega(t) + D(\omega)\omega(t) = \Pi(\omega, \dot{\omega})\Theta(t), \tag{11}$$

where $\Theta(t) \in \Re^p$ represents the vector of uncertain parameters and $\Pi(\omega, \dot{\omega}) \in \Re^{3\times p}$ is referred to as the dynamic regressor matrix that contains known parameters.

Remark 1 The above properties are logical because they are consistent with physical principles, mathematical requirements, and modeling practices commonly employed in fields like robotics, control theory, and mechanics [26–29]. They help simplify the representation and analysis of complex systems while adhering to fundamental principles.

3. Controller design

The principal objective of this paper is to formulate a robust adaptive control law for MSV, capable of handling uncertainties in both kinematics and dynamics.

As is well established [25], the system's state variables can be classified into two categories: fast time-varying variables, situated within the body-fixed frame, which encompass the MSV's velocities in surge, sway, and yaw directions; and slow time-varying variables, characterizing the MSV's position and orientation in the earth-fixed frame. To achieve this, we implement a double-loop control strategy for trajectory tracking. The outer loop at the kinematic level is dedicated to stabilizing the slow variables, while the inner loop at the dynamic level is focused on stabilizing the fast variables. The designed controller should ensure the overall stability of the system and maintain bounded signals within the closed-loop control system.

3.1. Design of the kinematic controller with ocean current estimation

In this subsection, our focus is on the design of an outer-loop-based kinematic control system, which aims to achieve precise tracking of the MSV's position and orientation, particularly in the presence of ocean currents. This controller generates velocity commands and is reinforced by the integration of an adaptive estimator. This estimator plays a crucial role in estimating and compensating for the unknown ocean current velocity, ultimately enhancing the performance and reliability of MSV operations in complex marine environments. Before commencing the synthesis of the control algorithm, it is essential to take into account the following assumptions.

Assumption 1 The reference posture $P_d(t)$ and its first derivative are continuous and time-varying within certain bounded limits, i.e., for all $t > 0$, there exist positive constants ℓ_1 and ℓ_2, such that $\|P_d(t)\| \leqslant \ell_1$ and $\left\|\dot{P}_d(t)\right\| \leqslant \ell_2$.

Assumption 2 The yaw angle $\Psi(t)$ is assured to stay within the specified limit as follows: $|\Psi(t)| < \pi/2$.

Assumption 3 The velocity of the ocean currents $\rho(t)$ is assumed to be time-varying and constrained over time by a positive bound, i.e., there exist $\varpi > 0$, such that $\|\rho(t)\| \leqslant \varpi$ for all $t > 0$.

Assumption 4 It is assumed that the environmental marine disturbances, potentially induced by factors such as ocean current velocity, wind, and waves, are presumed to vary slowly over time. More precisely, the time derivatives of these disturbances are assumed to be equal to zero.

Assumption 5 Information concerning the position(X, Y), orientation (Ψ), and velocities (u, v, r) of the MSV is typically accessible for feedback.

Remark 2 The yaw angle must not exceed 90° to establish overall effectiveness and safety in maritime operations. This constraint can be realized in practice by

achieving a balance between stability, maneuverability, and hydrodynamic performance. Hence, the transformation matrix $R(\Psi)$ is guaranteed to be nonsingular at all times.

Remark 3 Several factors contribute to ocean current formation, including winds, the Coriolis effect, temperature and density gradients, gravity, tidal forces, and underwater topography. For example, wind imparts surface momentum, the Coriolis effect guides current direction, and gravity, tidal forces, and ocean floor topography contribute to overall ocean water motion. The boundedness of ocean currents is logical as it aligns with the natural constraints imposed by earth's geography, climate system, and fundamental fluid dynamics laws.

Remark 4 Many marine environmental disturbances, such as ocean currents, wind patterns, and wave conditions, are influenced by large-scale physical processes. Observations and data from the real world show that these processes often change gradually over extended periods, resulting in slow variations in the associated disturbances. Therefore, Assumption 4 is completely logical.

Remark 5 To achieve precise navigation, control, and operation in diverse marine environments, it is essential to integrate sensors into the MSV to provide comprehensive data on the position, orientation, and velocity of the system. For example, these sensors may include GPS (Global Positioning System) for accurate location data, IMU (Inertial Measurement Unit) equipped with accelerometers and gyroscopes for tracking orientation and velocity changes, and compass/magnetometer for heading information.

Let's consider trajectory tracking missions, where the reference posture $P_d(t)$ is generated by a virtual MSV and adheres to the following equation:

$$\dot{P}_d(t) = \begin{bmatrix} \dot{X}_d(t) \\ \dot{Y}_d(t) \\ \dot{\Psi}_d(t) \end{bmatrix} = \begin{bmatrix} \cos\Psi_d & -\sin\Psi_d & 0 \\ \sin\Psi_d & \cos\Psi_d & 0 \\ 0 & 0 & 1 \end{bmatrix} \begin{bmatrix} u_d(t) \\ v_d(t) \\ r_d(t) \end{bmatrix}. \tag{12}$$

Therefore, we can define the so-called global posture error of the MSV in the earth-fixed frame as the disparity between the reference and current posture, as follows:

$$e_P(t) = P_d(t) - P(t) = \begin{bmatrix} e_X(t) \\ e_Y(t) \\ e_\Psi(t) \end{bmatrix} = \begin{bmatrix} X_d(t) - X(t) \\ Y_d(t) - Y(t) \\ \Psi_d(t) - \Psi(t) \end{bmatrix}. \tag{13}$$

In the body-fixed frame, we can define a local posture error of the MSV, which can be subsequently derived as follows:

$$P_e(t) = \begin{bmatrix} X_e(t) \\ Y_e(t) \\ \Psi_e(t) \end{bmatrix} = \begin{bmatrix} \cos\Psi & \sin\Psi & 0 \\ -\sin\Psi & \cos\Psi & 0 \\ 0 & 0 & 1 \end{bmatrix} \begin{bmatrix} e_X(t) \\ e_Y(t) \\ e_\Psi(t) \end{bmatrix} = R^T(\Psi) e_P(t). \tag{14}$$

Building upon Equation (4) and Equation (12), we can represent the time derivative of the local posture error through the following system:

$$\begin{aligned} \dot{X}_e &= rY_e + u_d \cos\Psi_e - v_d \sin\Psi_e - u - \rho_X \cos\Psi - \rho_Y \sin\Psi, \\ \dot{Y}_e &= -rX_e + u_d \sin\Psi_e + v_d \cos\Psi_e - v + \rho_X \sin\Psi - \rho_Y \cos\Psi, \\ \dot{\Psi}_e &= r_d - r. \end{aligned} \tag{15}$$

We will employ Lyapunov's stability theory to devise the kinematic control law for our system, with a particular focus on its effectiveness when influenced by ocean currents. Additionally, we will tackle the adaptation law, a crucial component intended to handle the kinematic disturbances introduced by these ocean currents. To fulfill this goal, we will employ the following Lyapunov candidate function:

$$V = \frac{1}{2} X_e^T X_e + \frac{1}{2} Y_e^T Y_e + \frac{1}{2} \Psi_e^T \Psi_e + \frac{1}{2} k_x \tilde{\rho}_X^2 + \frac{1}{2} k_y \tilde{\rho}_Y^2. \tag{16}$$

Here, $\tilde{\rho}_X = \rho_X - \hat{\rho}_X$ and $\tilde{\rho}_Y = \rho_Y - \hat{\rho}_Y$ represent the estimation errors of the ocean current velocity along the X_E-axis and Y_E-axis, respectively. These errors are defined as the difference between the actual and estimated velocities, with k_x and k_y denoting positive constants.

After taking the time derivative of the Lyapunov candidate function, we have:

$$\dot{V} = X_e \dot{X}_e + Y_e \dot{Y}_e + \Psi_e \dot{\Psi}_e + \frac{1}{k_x} \tilde{\rho}_X \dot{\tilde{\rho}}_X + \frac{1}{k_y} \tilde{\rho}_Y \dot{\tilde{\rho}}_Y. \tag{17}$$

When we substitute the local posture error (15) into the above equation, we obtain:

$$\begin{aligned} \dot{V} = {} & X_e \left(rY_e + u_d \cos\Psi_e - v_d \sin\Psi_e - u - \rho_X \cos\Psi - \rho_Y \sin\Psi \right) \\ & + Y_e \left(-rX_e + u_d \sin\Psi_e + v_d \cos\Psi_e - v + \rho_X \sin\Psi - \rho_Y \cos\Psi \right) \\ & + \Psi_e (r_d - r) + \frac{1}{k_x} \tilde{\rho}_X \dot{\tilde{\rho}}_X + \frac{1}{k_y} \tilde{\rho}_Y \dot{\tilde{\rho}}_Y. \end{aligned} \tag{18}$$

After replacing $\rho_X = \tilde{\rho}_X + \hat{\rho}_X$, $\rho_Y = \tilde{\rho}_Y + \hat{\rho}_Y$ and rearranging the above equation, we have:

$$\begin{aligned}\dot{V} = {} & X_e\Big(u_d\cos\Psi_e - v_d\sin\Psi_e - u - \hat{\rho}_X\cos\Psi - \hat{\rho}_Y\sin\Psi\Big)\\ & + \tilde{\rho}_X\Big(-X_e\cos\Psi + Y_e\sin\Psi + \frac{1}{k_x}\dot{\tilde{\rho}}_X\Big)\\ & + Y_e\Big(u_d\sin\Psi_e + v_d\cos\Psi_e - v + \hat{\rho}_X\sin\Psi - \hat{\rho}_Y\cos\Psi\Big)\\ & + \tilde{\rho}_Y\Big(-X_e\sin\Psi - Y_e\cos\Psi + \frac{1}{k_y}\dot{\tilde{\rho}}_Y\Big)\\ & + \Psi_e(r_d - r).\end{aligned} \tag{19}$$

To ensure the stability of the control law, it is essential that the time derivative of the candidate Lyapunov function is negative. Therefore, we need to consider the following two conditions:

$$\begin{aligned}u_d\cos\Psi_e - v_d\sin\Psi_e - u - \hat{\rho}_X\cos\Psi - \hat{\rho}_Y\sin\Psi &= -k_1X_e,\\ u_d\sin\Psi_e + v_d\cos\Psi_e - v + \hat{\rho}_X\sin\Psi - \hat{\rho}_Y\cos\Psi &= -k_2Y_e,\\ r_d - r &= -k_3\Psi_e,\end{aligned} \tag{20}$$

and:

$$\begin{aligned}-X_e\cos\Psi + Y_e\sin\Psi + \frac{1}{k_x}\dot{\tilde{\rho}}_X &= 0,\\ -X_e\sin\Psi - Y_e\cos\Psi + \frac{1}{k_y}\dot{\tilde{\rho}}_Y &= 0,\end{aligned} \tag{21}$$

where k_1 , k_2 and k_3 are positive scalars.

From condition (20), we can deduce the following kinematic adaptive law:

$$\boldsymbol{\omega}_c(t) = \begin{bmatrix}u_c(t)\\ v_c(t)\\ r_c(t)\end{bmatrix} = \begin{bmatrix}k_1X_e + u_d\cos\Psi_e - v_d\sin\Psi_e - \hat{\rho}_X\cos\Psi - \hat{\rho}_Y\sin\Psi\\ k_2Y_e + u_d\sin\Psi_e + v_d\cos\Psi_e + \hat{\rho}_X\sin\Psi - \hat{\rho}_Y\cos\Psi\\ k_3\Psi_e + r_d\end{bmatrix}. \tag{22}$$

Assumption 4 states that the ocean current velocity varies slowly over time, which means that $\dot{\rho} = 0$. Consequently, the adaptation law for the unknown ocean current velocity can be derived from (21) as follows:

$$\begin{aligned}\dot{\hat{\rho}}_X &= k_x\left(-X_e\cos\Psi + Y_e\sin\Psi\right),\\ \dot{\hat{\rho}}_Y &= k_y\left(-X_e\sin\Psi - Y_e\cos\Psi\right).\end{aligned} \tag{23}$$

After applying the suggested control law (22) along with the adaptation law for the ocean current velocity (23), the time derivative of the Lyapunov candidate function is simplified to:

$$\dot{V} = -k_1X_e^2 - k_2Y_e^2 - k_3\Psi_e^2 \geqslant 0. \tag{24}$$

Given that $V \geqslant 0$ and $\dot{V} \leqslant 0$, it is evident that V is a bounded function and has a finite limit as time goes to infinity. This implies that V is bounded, and

consequently, its components, including the tracking errors X_e, Y_e, and Ψ_e, as well as the estimation errors $\tilde{\rho}_X$ and $\tilde{\rho}_Y$, are also bounded. Furthermore, assuming that the reference posture X_d, Y_d, and Ψ_d is bounded (as per Assumption 1), we can deduce from equation (14) that the actual posture X, Y, and $\Psi$are also bounded. The boundedness of reference posture and desired posture implies, from equations (4) and (12), the boundedness of the reference and actual velocity, i.e., u_d, v_d, r_d, u, v, and r. Similarly, relying on Assumption 3 and considering that actual ocean currents ρ_X and ρ_Y are bounded, and given that the errors in estimating these currents $\tilde{\rho}_X$ and $\tilde{\rho}_Y$ are also bounded, we can infer that the estimated ocean currents $\hat{\rho}_X$ and $\hat{\rho}_Y$ are likewise bounded. Based on the previous analysis, we can affirm that the kinematic control law (22) and update law (23) for the ocean currents are bounded. After all, we can affirm that all signals of the closed-loop system are bounded. Furthermore, the second time derivative of the Lyapunov function can be computed as $\ddot{V} = -2k_1 X_e \dot{X}_e - 2k_2 Y_e \dot{Y}_e - 2k_3 \Psi_e \dot{\Psi}_e$. Equation (15) can demonstrate the boundedness of $\dot{X}_e$, $\dot{Y}_e$, and $\dot{\Psi}_e$, and given the boundedness of X_e, Y_e, and Ψ_e, we can assert the boundedness of $\ddot{V}$, implying that $\dot{V}$ is uniformly continuous. By applying the Barbalat Lemma, we can conclude that $\lim_{t\to\infty} V(t) = 0$, and consequently, $\lim_{t\to\infty} X_e(t) = 0$; $\lim_{t\to\infty} Y_e(t) = 0$; $\lim_{t\to\infty} \Psi_e(t) = 0$; $\lim_{t\to\infty} \tilde{\rho}_X(t) = 0$ and $\lim_{t\to\infty} \tilde{\rho}_Y(t) = 0$, which finally implies that $X(t) \to X_d(t)$, $Y(t) \to Y_d(t)$, $\Psi(t) \to \Psi_d(t)$, $\rho_X(t) \to \hat{\rho}_X(t)$ and $\rho_Y(t) \to \hat{\rho}_Y(t)$ when time goes to infinity. This completes the proof of the asymptotic convergence.

The previous analysis can be summarized in the following theorem:

Theorems 1 Consider the MSV system governed by the kinematic Equation (4) in the presence of unknown ocean currents, assuming that Assumptions 1–5 are satisfied. If the velocity command in Equation (22) is designed in the outer loop, incorporating the update laws for the estimation of ocean currents in Equation (23), then, for any initial posture and smooth reference trajectory, the following conditions hold:

1. The posture tracking errors converge asymptotically to zero.
2. The estimation error for unknown ocean currents converges to a small neighborhood around the origin.
3. All signals of the outer-loop system are uniformly ultimately bounded.

Remark 6 In this study, the estimation of ocean current velocity has been solely based on position measurements, which represents a significant advancement in marine sensing techniques. By utilizing position data, this approach demonstrates an innovative method for deriving crucial information about ocean currents. Such innovation not only underscores the ingenuity of the estimation process but also holds promise for cost-effective and accessible solutions in oceanography, offering a valuable tool for understanding and monitoring marine dynamics.

3.2. Design of the dynamic controller with parameters and disturbances estimation

In this subsection, our focus is on the design of an inner-loop-based dynamic control system, which aims to achieve precise tracking of the MSV velocity, especially in the presence of uncertain dynamic parameters and external torque disturbances. This controller generates input torque and is strengthened by the integration of adaptive estimators for unknown parameters and external disturbances, using only information about the position and velocity of the system. These estimators contribute significantly to improving the efficiency and dependability of the MSV operations in completely unknown dynamic parameters and severe marine disturbances, which may arise from wind, waves, etc.

It is necessary to consider the following Assumptions before starting to synthesize the control algorithm.

Assumption 6 The external disturbance $\Delta(t)$ is assumed to be time-varying, inherently unmeasurable, and yet bounded, i.e., there exist $\delta > 0$, such that $\|\Delta(t)\| \leqslant \delta$ for all $t > 0$.

Assumption 7 The dynamic parameters M, $C(\omega)$ and $D(\omega)$ of the MSV are assumed to completely unknown but there are bounded.

Remark 7 The external disturbances in marine environments arise from factors such as ocean currents, wind patterns, and wave conditions, contributing to the dynamic nature of the system. The assumption that these disturbances are unmeasurable is based on the complex and vast scales of marine systems, making precise measurements challenging. Additionally, the finite time energy of marine disturbances contributes to the boundedness of the disturbance by imposing constraints on its overall magnitude and variability.

Remark 8 The dynamic parameters of MSV, including added mass, inertia, and hydrodynamic parameters, are associated with vehicle characteristics, maneuvers, and environmental conditions. The characterization of these parameters as unknown arises from the intricate and variable nature of the marine environment, the complexity of hydrodynamics, and practical challenges in measurement. Despite their unknown nature, it is assumed that these dynamic parameters remain within certain limits due to practical considerations and the physical limitations imposed by the marine environment.

To begin, let's define the velocity tracking error, which is the difference between the commanded velocity generated by the kinematic algorithm and the actual velocity, as follows:

$$e_{\omega}(t) = \omega_c(t) - \omega(t). \tag{25}$$

The following classical computed torque input can be designed to ensure the convergence of the actual velocity ω to the velocity command ω_c [25], as given by the following equation:

$$\Gamma(t) = M\dot{\omega}_c(t) + C(\omega)\omega_c(t) + D(\omega)\omega(t) + Ke_\omega(t), \tag{26}$$

where K is a positive gain matrix.

The accurate tracking performance of the above controller is assured only if the dynamic quantities M,$C(\omega)$, $D(\omega)$ are perfectly known. However, obtaining this information is challenging due to the complexity of measuring or estimating the hydrodynamic parameters of the MSV. Additionally, marine torque disturbances arising from various environmental factors such as wind, waves, and tides can impact the normal operation or behavior of marine systems, potentially leading to system instability. Consequently, effective control systems are often necessary to mitigate these effects and ensure the reliable execution of missions. To address these challenges, the computed torque controller in Equation (26) can be enhanced as follows:

$$\Gamma(t) = \hat{M}\dot{\omega}_c(t) + \hat{C}(\omega)\omega_c(t) + \hat{D}(\omega)\omega(t) + Ke_\omega(t) - \hat{\Delta}(t), \tag{27}$$

where the matrices $\hat{M}$, $\hat{C}(\omega)$ and $\hat{D}(\omega)$ are the estimates of M, $C(\omega)$, and $D(\omega)$ respectively, and $\hat{\Delta}(t)$ is the estimate of the unknown disturbance torque $\Delta(t)$.

Utilizing the linear parametrizable Property 3, Equation (27) can be expressed in the following concise form:

$$\Gamma(t) = \Pi(\omega, \omega_c, \dot{\omega}_c)\hat{\Theta}(t) + Ke_\omega(t) - \hat{\Delta}(t), \tag{28}$$

where $\hat{\Theta} \in \Re^9$ represents the estimated vector of unknown dynamic parameters. We note the existence of 9 unknown dynamic parameters for the system, which can be grouped together in the following vector:

$$\Theta = \left[m_{11} \quad m_{22} \quad m_{23} \quad m_{33} \quad d_{11}(u) \quad d_{22}(v,r) \quad d_{23}(v,r) \quad d_{32}(v,r) \quad d_{33}(v,r). \right]^T \tag{29}$$

The terms Π_{ij} $(i = 1 \sim 3, j = 1 \sim 9)$ of the regression matrix $\Pi(\omega, \omega_c, \dot{\omega}_c)$ can be determined as follows: first, calculate the vector $\Upsilon = \left[\begin{array}{ccc} \Upsilon_1 & \Upsilon_2 & \Upsilon_3 \end{array} \right]^T \in \Re^3$ such that $\Upsilon = M\dot{\omega}_c + C(\omega)\omega_c + D(\omega)\omega$, after which we find that:

$$\begin{aligned}
\Upsilon_1 =& \dot{u}_c m_{11} - v r_c m_{22} - r r_c m_{23} + u d_{11}(u), \\
\Upsilon_2 =& u r_c m_{11} + \dot{v}_c m_{22} + \dot{r}_c m_{23} + v d_{22}(v,r) + r d_{23}(v,r), \\
\Upsilon_3 =& -u v_c m_{11} + u_c v m_{22} + (\dot{v}_c + u_c r) m_{23} + \dot{r}_c m_{33} + v d_{32}(v,r) + r d_{33}(v,r).
\end{aligned}$$

Then, for $j = 1 \sim 9$, we have: $\Pi_{1j} = \dfrac{\partial \Upsilon_1}{\partial \Theta_i}$; $\Pi_{2j} = \dfrac{\partial \Upsilon_2}{\partial \Theta_i}$; $\Pi_{3j} = \dfrac{\partial \Upsilon_3}{\partial \Theta_i}$.

Finally, after these calculations, the measurable regression matrix $\Pi(\omega, \omega_c, \dot{\omega}_c) \in \Re^{3\times 9}$ can be computed as follow:

$$\Pi(\omega, \omega_c, \dot{\omega}_c) = \begin{bmatrix} \dot{u}_c & -vr_c & -rr_c & 0 & u & 0 & 0 & 0 & 0 \\ ur_c & \dot{v}_c & \dot{r}_c & 0 & 0 & v & r & 0 & 0 \\ -uv_c & u_c v & \dot{v}_c + u_c r & \dot{r}_c & 0 & 0 & 0 & v & r \end{bmatrix}. \tag{30}$$

By substituting the control law provided in Equation (27) into the dynamic model expressed in Equation (5), we derive the dynamic behavior of the closed-loop system as follows:

$$M\dot{e}_\omega + C(\omega)e_\omega + Ke_\omega - \Pi(\omega, \omega_c, \dot{\omega}_c)\tilde{\Theta} + \tilde{\Delta} = 0, \tag{31}$$

where $\tilde{\Theta} = \Theta - \hat{\Theta}$ defines the parameter estimation error, while $\tilde{\Delta} = \Delta - \hat{\Delta}$ represents the estimation errors associated with external disturbances.

We will use Lyapunov's stability theory to design the dynamic control law for our system, paying specific attention to its effectiveness in the presence of unknown dynamic parameters. Furthermore, we will address the adaptation law, a critical component designed to manage external disturbances. To achieve this objective, we will utilize the following Lyapunov candidate function:

$$V = \frac{1}{2}e_\omega^T M e_\omega + \frac{1}{2}\tilde{\Theta}^T K_\Theta \tilde{\Theta} + \frac{1}{2}\tilde{\Delta}^T K_\Delta \tilde{\Delta}, \tag{32}$$

where K_Θ and K_Δ are diagonal positive definite matrices.

After taking the time derivative of the Lyapunov candidate function, we have:

$$\dot{V} = e_\omega^T M\dot{e}_\omega + \frac{1}{2}e_\omega^T \dot{M} e_\omega + \tilde{\Theta}^T K_\Theta \dot{\tilde{\Theta}} + \tilde{\Delta}^T K_\Delta \dot{\tilde{\Delta}}. \tag{33}$$

The substitution of the closed-loop behavior (31) in the above equation, followed by the application of the skew-symmetric Property 2, results in:

$$\dot{V} = -e_\omega^T K e_\omega + \left(e_\omega^T \Pi(\omega, \omega_c, \dot{\omega}_c) + \dot{\tilde{\Theta}}^T K_\Theta\right)\tilde{\Theta} + \left(-e_\omega^T + \dot{\tilde{\Delta}}^T K_\Delta\right)\tilde{\Delta}. \tag{34}$$

To ensure the stability of the control law, it is essential that the time derivative of the candidate Lyapunov function is negative. Therefore, we need to consider the following two conditions:

$$e_\omega^T \Pi(\omega, \omega_c, \dot{\omega}_c) + \dot{\tilde{\Theta}}^T K_\Theta = 0, \tag{35}$$

and:

$$-e_\omega^T + \dot{\tilde{\Delta}}^T K_\Delta = 0. \tag{36}$$

Based on the Assumption 4 that the variable changes slowly over time, i.e., $\dot{\tilde{\Theta}} = -\dot{\hat{\Theta}}$ and $\dot{\tilde{\Delta}} = -\dot{\hat{\Delta}}$, then the adaptation law for the unknown dynamic parameters is given by:

$$\dot{\hat{\Theta}} = K_{\Theta}^{-T} \Pi^{T} \left(\omega, \omega_c, \dot{\omega}_c\right) e_{\omega}. \tag{37}$$

Similarly, the adaptation law for the external disturbance torque is as follows:

$$\dot{\hat{\Delta}} = -K_{\Delta}^{-T} e_{\omega}. \tag{38}$$

After applying the suggested control law (28) along with the adaptation law for the unknown dynamic parameters (37) and the adaptation law for the external disturbance torque (38), the time derivative of the Lyapunov candidate function is simplified to:

$$\dot{V} = -e_{\omega}^{T} K e_{\omega} \leqslant 0. \tag{39}$$

Given that $V \geqslant 0$ and $\dot{V} \leqslant 0$, it is evident that V is a bounded function and has a finite limit as time goes to infinity. This implies that V is bounded, and consequently, its components, including the velocity error e_{ω}, as well as the estimation errors for the dynamic parameters and external disturbances $\tilde{\Theta}$ and $\tilde{\Delta}$, are also bounded. Using the fact that the velocity command ω_c, is bounded, we can deduce that the actual velocity ω is also bounded. Relying on Assumptions 6, 7 and considering that dynamic parameters Θ and external disturbances Δ are bounded, and given that the errors in estimating these variables $\tilde{\Theta}$ and $\tilde{\Delta}$ are also bounded, we can infer that their estimated values $\hat{\Theta}$ and $\hat{\Delta}$ are likewise bounded. Based on the previous analysis, we can affirm that the dynamic control law (28) and the update laws (37) and (38) for the dynamic parameters and external disturbances are bounded. After all, we can affirm that all signals of the closed-loop system are bounded. Furthermore, the second time derivative of the Lyapunov function can be computed as $\ddot{V} = -2\dot{e}_{\omega}^{T} K e_{\omega}$. We can affirm the boundedness of $\ddot{V}$, implying that $\dot{V}$ is uniformly continuous. By applying the Barbalat Lemma, we can conclude that $\lim\limits_{t\to\infty} V(t) = 0$, and consequently, $\lim\limits_{t\to\infty} e_{\omega}(t) = 0$; $\lim\limits_{t\to\infty} \tilde{\Theta}(t) = 0$ and $\lim\limits_{t\to\infty} \tilde{\Delta}(t) = 0$, which finally implies that $\omega(t) \to \omega_c(t)$, $\Theta(t) \to \hat{\Theta}(t)$ and $\Delta(t) \to \hat{\Delta}(t)$ when time goes to infinity. This completes the proof of the asymptotic convergence.

The previous analysis can be summarized in the following theorem:

Theorems 2 Consider the MSV system governed by the dynamic Equation (5) in the presence of unknown dynamic parameters and external torque disturbances, assuming that Assumptions 6–7 are satisfied. If the input torque in Equation (28) is designed in the inner loop, incorporating the update laws for the unknown dynamic parameters in Equation (37) and for external torque disturbances in Equation (38), then, for any smooth velocity command, the following conditions hold:

1. The velocity tracking errors converge asymptotically to zero.

2. The estimation error for unknown dynamic parameters and external torque disturbances converges to a small neighborhood around the origin.
3. All signals of the inner-loop system are uniformly ultimately bounded.

The schema bloc of the overall double-loop controller is illustrated in Fig. 2.

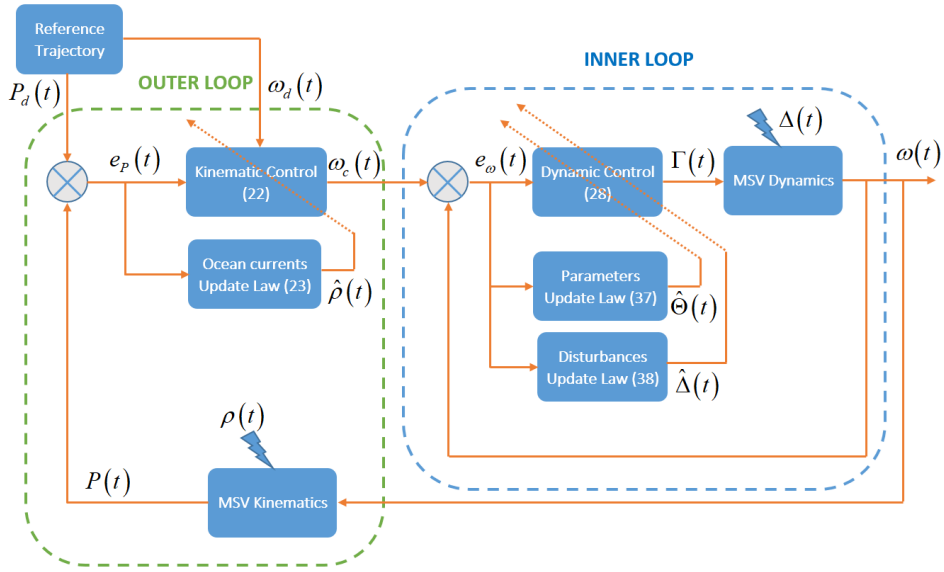

Fig. 2. Block diagram of the proposed double-loop controller

Remark 9 The assumption that variables change slowly over time is often made in adaptive control for practical reasons and to simplify the design of control systems. This assumption is logical in marine missions due to natural constraints, dynamic conditions, safety considerations, and energy efficiency requirements inherent in maritime systems. Embracing this assumption enables smoother adjustments, reduces the risk of instability, and aligns with the efficient use of propulsion systems, especially in the face of environmental challenges.

Remark 10 In adaptive control systems, parameter drift can occur due to uncertainties and disturbances, causing the adaptive parameters to increase without bound, which undermines the accuracy and stability of the controller. To address this, the dead-zone technique is applied by introducing a threshold around zero that prevents unnecessary parameter updates when the error is small. Specifically, the update law for the adaptive parameters is modified such that if the error magnitude is below a predefined threshold , no update occurs, while the parameter update is governed by an adaptive law when the error exceeds . This approach ensures that only significant errors trigger adaptations, stabilizing the control system and preventing unnecessary drift [39–41].

Remark 11 In designing the proposed dual-loop algorithm, it is essential to follow a systematic approach to ensure optimal performance and stability. The following steps outline the process for selecting and refining the controller gain parameters:

Step 1: Define the Inputs

- Specify the desired trajectory $P_d(t)$: This trajectory outlines the target path, including both position and orientation over time, that the system should follow.
- Measure the actual trajectory $P(t)$: The system's real-time trajectory is recorded to provide feedback, allowing for continuous comparison with the desired path.
- Examine the system model to understand the dynamics that affect control inputs, which is essential for estimating parameters and defining error terms.

Step 2: Design the Adaptive Kinematic Controller with Ocean Current Estimation

- Compute the global posture error $e_P(t) = P_d(t) - P(t)$, which represents the difference between the desired and actual trajectories in the global reference frame.
- Compute the local posture error $P_e(t)$, a relative error used to refine the system's position and orientation alignment with the desired trajectory.
- Select the gains for the ocean current update laws: k_x and k_y are selected to allow for accurate estimation of ocean currents impacting the system.
- Select the gains for the kinematic controller: k_1, k_2, and $k_3$are chosen to improve tracking accuracy in both position and orientation.
- Design the adaptive kinematic controller as detailed in Equation (22), with update laws to estimate the ocean current (Equation (23)).

Step 3: Design the Adaptive Dynamic Controller with Parameter and Disturbance Estimation

- Compute the velocity tracking error $e_\omega(t)$ as the difference between velocities command and actual velocities, which refines accuracy in tracking the velocity command.
- Select gains for the parameter update law K_Θ, which adjusts the estimates of dynamic parameter $\Theta(t)$ for improved model alignment.
- Select gains for the disturbance update law K_Δ to mitigate the effects of unknown disturbances $\Delta(t)$ that can impact control performance.
- Design the adaptive dynamic controller as described in Equation (28), using parameter update laws (Equation (37)) and disturbance update laws (Equation (38)).

Step 4: Simulation and Refinement

- Simulate the controller with initial gains in a controlled environment, introducing variations in ocean current and external disturbances to observe the system's response.

- Adjust gains iteratively based on the simulation results to meet specific performance criteria, such as minimizing tracking error and optimizing response time.

Step 5: Final Evaluation

- Evaluate tracking performance against pre-established criteria. If the results are satisfactory, the gains are finalized.
- If necessary, return to Steps 2 and 3 for further gain refinement.

4. Simulation results

In this subsection, extensive computer simulations will be conducted to verify the effectiveness of the proposed controller. For this purpose, we use the MSV *Northern Gripper* as a simulation example. This vessel, which is a giant in terms of its size and equipped with powerful thrusters, has a length of 76.2 m long and a mass of $4.591.10^6$ kg. The torque ranges that the MSV's actuators can support are as follows: $\Gamma_u \in \left[-2.5.10^3;\ 2.5.10^3\right]$ kN, $\Gamma_v \in \left[-1.5.10^3;\ 1.5.10^3\right]$ kN, and $\Gamma_r \in \left[-2.10^5;\ 2.10^5\right]$ kNm. For more detailed information on the hydrodynamic parameters of the MSV, please refer to [42, 43].

The desired trajectory to be followed is planned as follows:

$$P_d(t) = \begin{bmatrix} X_d(t) \\ Y_d(t) \\ \Psi_d(t) \end{bmatrix} = \begin{bmatrix} 600\cos(0.72t)\cos(0.12t) \\ 600\cos(0.72t)\sin(0.12t) \\ 60\sin(0.1t) \end{bmatrix}. \tag{40}$$

To verify the robustness of our control system, we considered parametric uncertainties of 20% for the physical and hydrodynamic parameters relative to their nominal values. Additionally, we took into account the following marine environment disturbance [36]:

$$\Delta(t) = \begin{bmatrix} \Delta_u(t) \\ \Delta_v(t) \\ \Delta_r(t) \end{bmatrix} = \begin{bmatrix} 10^4\left(\sin(0.2t) + \cos(0.5t)\right) + \delta(t) \\ 10^4\left(\sin(0.1t) + \cos(0.4t)\right) + \delta(t) \\ 10^4\left(\sin(0.5t) + \cos(0.3t)\right) + \delta(t) \end{bmatrix}, \tag{41}$$

where $\delta(t) = \aleph(0, 1)$ represents a white Gaussian noise with an amplitude of 0.1 and a sample time of 0.001 seconds.

We have also considered the following kinematic disturbance arising from the velocity of ocean currents:

$$\rho(t) = \begin{bmatrix} \rho_X(t) \\ \rho_Y(t) \\ 0 \end{bmatrix} = \begin{bmatrix} 2\sin(0.4t) \\ 2\cos(0.4t) \\ 0 \end{bmatrix}. \tag{42}$$

The initial configuration of the MSV is set to $P(0) = [5 \quad -4 \quad \pi/4]^T$, and its initial velocity is set to $\omega(0) = [0 \ 0 \ 0]^T$. The control gains are selected as $k_1 = 60$, $k_2 = 60$, $k_3 = 90$, $k_x = 700$, $k_y = 700$, $K = 900$, $K_\Theta = 1800$ and $K_\Delta = 1000$. The initial values of the adaptive parameters are assumed to be zero, i.e., $\hat{\rho}_X(0) = \hat{\rho}_Y(0) = 0$ and $\hat{\Theta}_i(0) = 0$ for $i = 1 \sim 9$. The tracking performances under these conditions are illustrated in Figs. 3–9.

Fig. 3 illustrates the impressive precision of the MSV as it adeptly follows a predetermined trajectory in the XY plane. The track showcases the advanced navigation capabilities of the system, highlighting its ability to maintain accurate and consistent tracking throughout the designated path. In Fig. 4, a comprehensive depiction of the temporal evolution of both positions X and Y, as well as the orientation Ψ, clearly demonstrates the effectiveness of the control mechanism in accurately steering the system along the intended path and underscores the overall reliability of the system in achieving precise and consistent positioning and orientation.

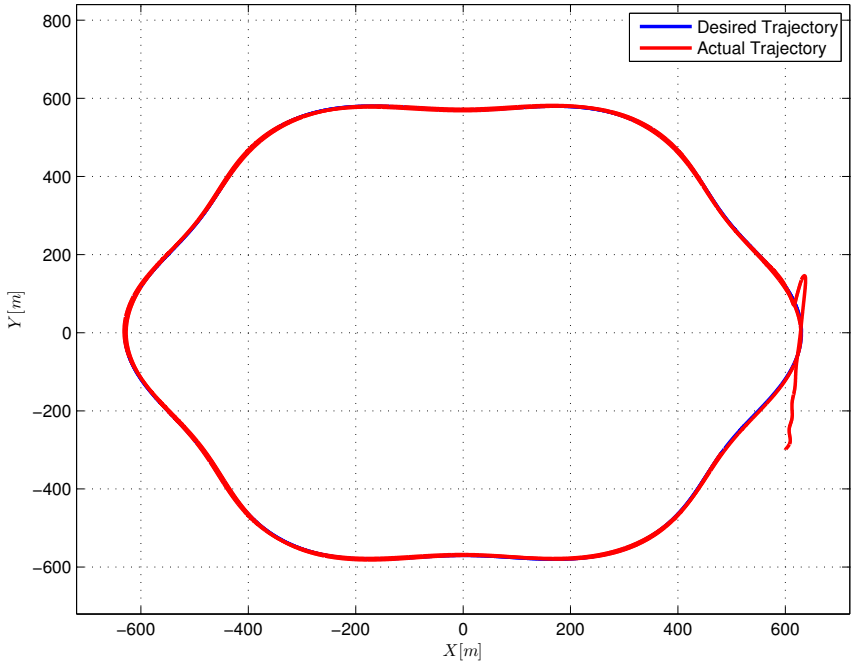

Fig. 3. Plot of the MSV tracking trajectory in the XY plane

The high tracking precision is further confirmed through the plot of the tracking errors in Fig. 5, which, after a transient due to errors in the initial condition, exhibit a small value and converge to zero. The good performance in position and orientation tracking is mainly attributed to the efficiency of the algorithm designed for estimating the current ocean velocity. As illustrated in Fig. 6, a perfect estimation

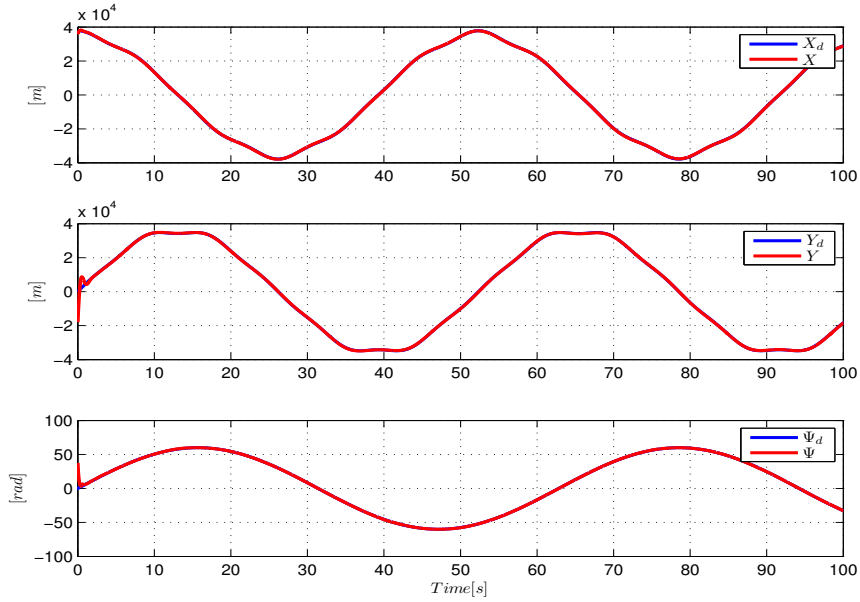

Fig. 4. Evolution of the position X , position Y , and orientation Ψ versus time

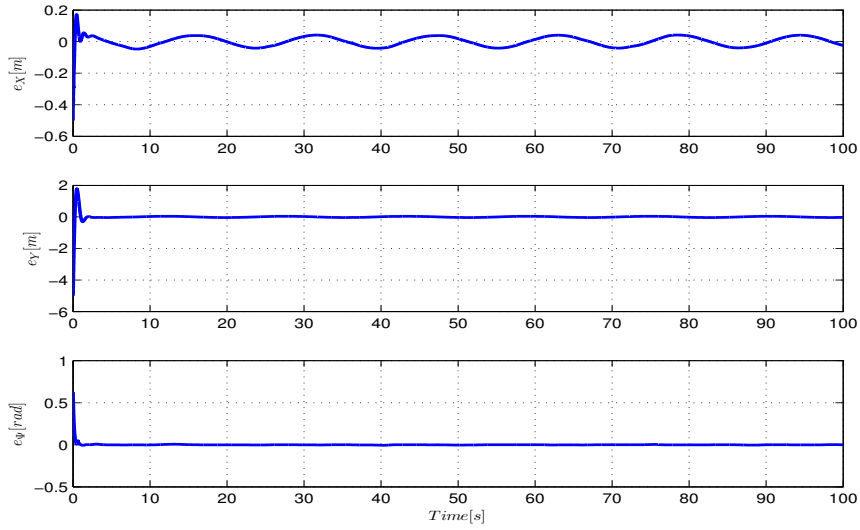

Fig. 5. Evolution of the tracking error in the X direction, Y direction, and heading

is achieved, and it can be observed that the estimated ocean current velocities align closely with the real ones. It is important to note that this estimation is achieved using only information data about the system's posture. This not only highlights the estimating process's creativity but also shows a cost-effective and potential tool for studying maritime dynamics. Furthermore, as shown in Fig. 7, it can be observed

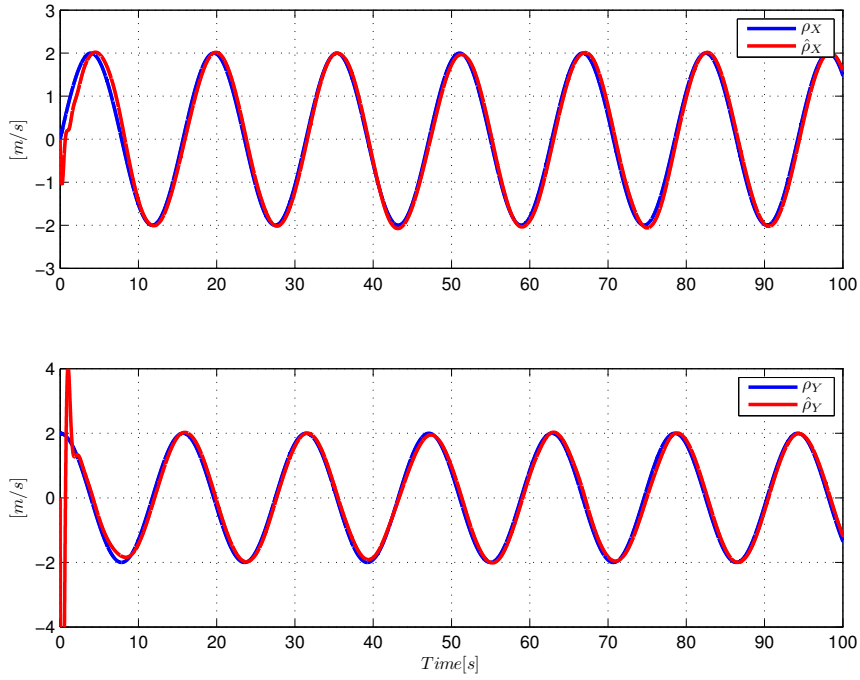

Fig. 6. Evolution of the estimated ocean current velocities versus time

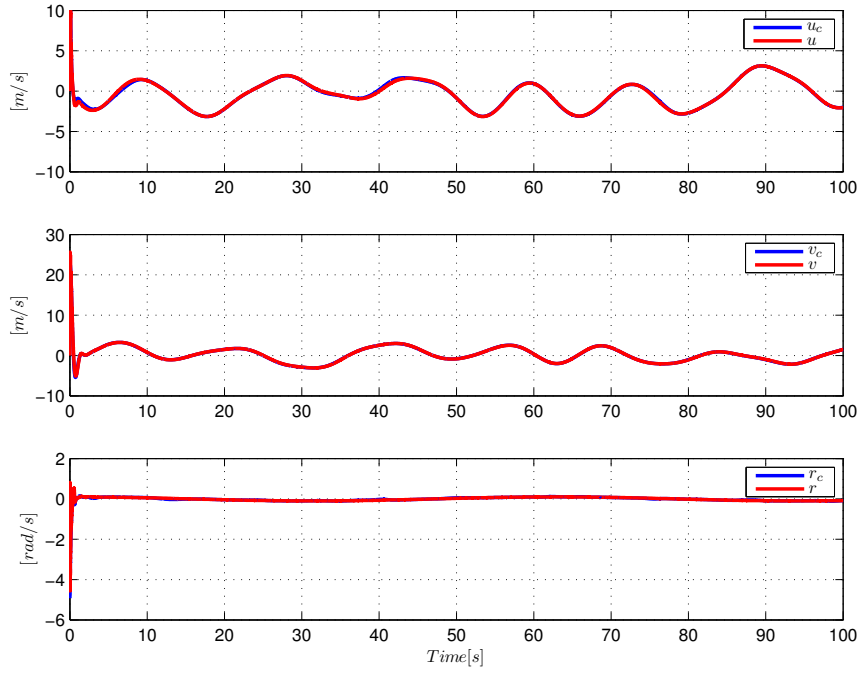

Fig. 7. Plot of the velocities command and actual velocities

that the actual velocities closely match the velocity commands generated by the kinematic controller, thereby demonstrating the validity of the proposed inner loop control.

The high speed at the beginning of the movement is a result of the initial conditions assumed in the simulation. Specifically, the model begins with a scenario where the vehicle is assumed to start with sufficient propulsion to achieve near-instantaneous acceleration to a higher speed. In the later stages of the simulation, the speed values become more realistic because the vehicle has reached its operational phase, where the dynamics are dominated by realistic interactions between propulsion, resistance, and environmental factors. This transition to realistic conditions reflects the system's equilibrium in real-world scenarios.

Fig. 8 shows the control signals of the actuators throughout the tracking control process. It can be observed that the signals remain smooth, with no signs of singularities or chattering. Furthermore, the torque and thrust values in the simulation now align more closely with the technical limitations of the MSV Northern Gripper, ensuring that the controller operates within realistic, feasible limits. As a result, the control signals reflect stable and realistic actuator performance, which is consistent with the vessel's actual capabilities. Fig. 9 shows the evolution of the adaptive parameters for the unknown dynamics; it can be seen that all the parameters converge rapidly to constant values after a brief oscillating period at the beginning. This confirms the ability of this algorithm to approximate unknown

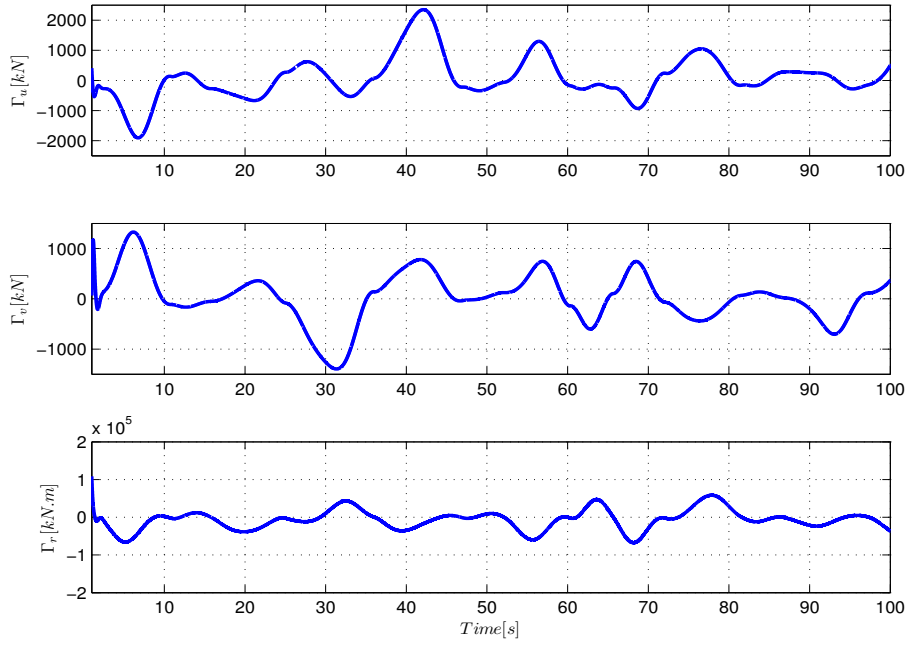

Fig. 8. Plot of the input torques

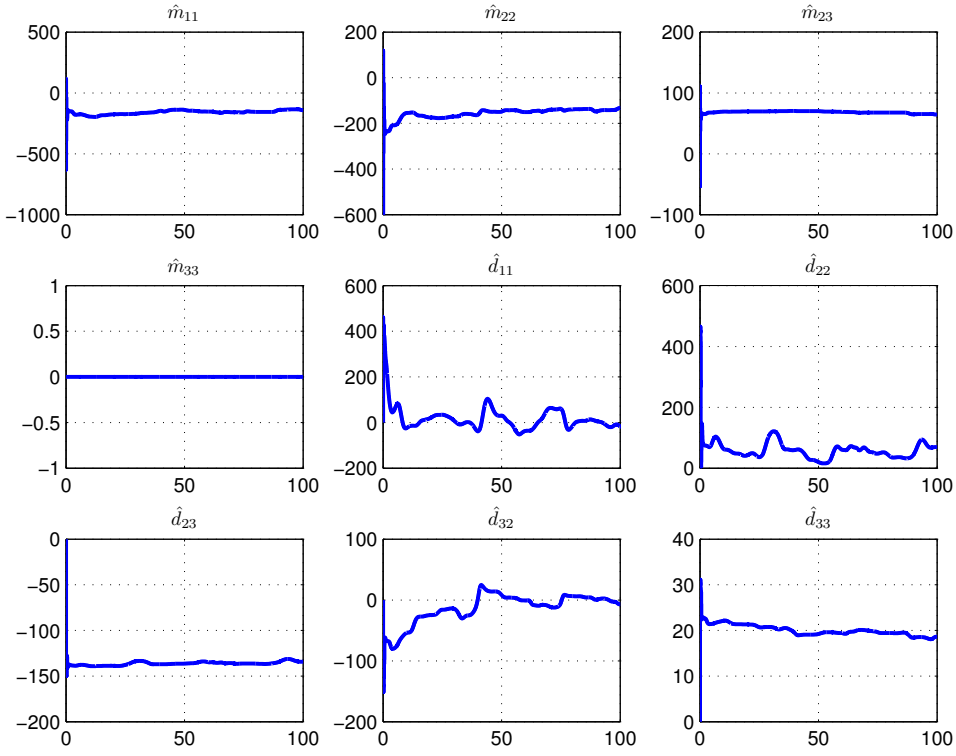

Fig. 9. Evolution of the estimated dynamic parameters versus time

dynamic parameters, which is useful in many practical situations. Notice that the observed consistency in input torques, despite significant variations in current speed, underscores the robustness of the proposed control system in compensating for disturbances caused by ocean currents. The adaptive estimator integrated into the outer-loop control effectively identifies and mitigates these disturbances, ensuring that the MSV maintains its desired trajectory and velocity even under fluctuating environmental conditions. This compensation mechanism minimizes the need for substantial adjustments in the inner-loop torque commands, enabling smooth operation without drastic changes in torque inputs. As a result, the input torques exhibit a stable system response, even amidst varying current conditions. This stability is a direct result of the effective disturbance rejection embedded in the control process, highlighting the system's reliability and adaptability.

5. Conclusions

This paper presents an adaptive control strategy for trajectory tracking of a Marine Surface Vehicle (MSV), accounting for parameter uncertainties, external disturbances, and ocean currents. The control system is designed with a double-

loop structure: an outer kinematic controller that generates velocity commands and an inner dynamic controller that provides real-time control inputs. The kinematic controller is enhanced with an adaptive algorithm to estimate and compensate for kinematic disturbances, particularly those caused by ocean currents. The dynamic controller is strengthened by two adaptive control laws: one for estimating unmeasured hydrodynamic parameters and another for compensating external disturbance torques. The overall stability of the closed-loop system is proven using Lyapunov stability theory. Simulation results confirm the robustness of the controller. The proposed control strategy demonstrates high tracking accuracy, strong robustness to disturbances, and effective compensation for ocean currents. It also ensures smooth and realistic actuator control. The system adapts well to parametric uncertainties and kinematic disturbances, with adaptive parameters converging to constant values. Despite its advantages, the strategy faces challenges in computational complexity, tuning, and potential higher implementation costs. Further validation in real-world conditions is necessary to evaluate its scalability and practical applicability.

References

[1] M.J. Er, C. Ma, T. Liu, and H. Gong. Intelligent motion control of unmanned surface vehicles: A critical review. *Ocean Engineering*, 280:114562, 2023. doi: 10.1016/j.oceaneng.2023.114562.

[2] X. Zhang, C. Wang, L. Jiang, L. An, and R. Yang. Collision-avoidance navigation systems for maritime autonomous surface ships: A state of the art survey. *Ocean Engineering*, 235:109380, 2021. doi: 10.1016/j.oceaneng.2021.109380.

[3] Z. Liu, Y. Zhang, X. Yu, and C. Yuan. Unmanned surface vehicles: An overview of developments and challenges. *Annual Reviews in Control*, 41:71–93, 2016. doi: 10.1016/j.arcontrol.2016.04.018.

[4] J. Ning, Y. Wang, E. Wang, L. Liu, C. L. Philip Chen, and S. Tong. Fuzzy trajectory tracking control of under-actuated unmanned surface vehicles with ocean current and input quantization. *IEEE Transactions on Systems, Man, and Cybernetics: Systems*, 55:63–72, 2025. doi: 10.1109/TSMC.2024.3460370.

[5] C. Sun, J. Liu, and J. Yu. Improved adaptive fuzzy control for unmanned surface vehicles with uncertain dynamics using high-power functions. *Ocean Engineering*, 312(2):119168, 2024. doi: 10.1016/j.oceaneng.2024.119168.

[6] X. Gao, Y. Long, T. Li, X. Hu, C. L. Philip Chen, and F. Sun. Optimal fuzzy output feedback control for dynamic positioning of vessels with finite-time disturbance rejection under thruster saturations. *IEEE Transactions on Fuzzy Systems*, 31(10):3447–3458, 2023. doi: 10.1109/TFUZZ.2023.3257200.

[7] S. Dong, K. Liu, M. Liu, G. Chen, and T. Huang. Adaptive neural network-quantized tracking control of uncertain unmanned surface vehicles with output constraints. *IEEE Transactions on Intelligent Vehicles*, 9(2):3293–3304, 2024. doi: 10.1109/TIV.2023.3331905.

[8] W. Wu, Z. Peng, D. Wang, L. Liu, and Q. L. Han. Network-based line-of-sight path tracking of underactuated unmanned surface vehicles with experiment results. *IEEE Transactions on Cybernetics*, 52(10):10937–10947, 2022. doi: 10.1109/TCYB.2021.3074396.

[9] H. Liu, X. Zhou, X. Tian, Q. Mai, and R. Li. Adaptive self-structuring neural network tracking control for underactuated USVs with actuator faults and input saturation. *Ocean Engineering*, 309(2):118535, 2024. doi: 10.1016/j.oceaneng.2024.118535.

[10] Y.L. Wang, C.C. Wang, Q.L. Han, and X. Wang. Networked and deep reinforcement learning-based control for autonomous marine vehicles: A survey. *IEEE Transactions on Systems, Man, and Cybernetics: Systems*, 55:4–17, 2025. doi: 10.1109/TSMC.2023.3346401.

[11] Z. Peng, E. Liu, C. Pan, H. Wang, D. Wang, and L. Liu. Model-based deep reinforcement learning for data-driven motion control of an under-actuated unmanned surface vehicle: Path following and trajectory tracking. *Journal of the Franklin Institute*, 360(6):4399–4426, 2023. doi: 10.1016/j.jfranklin.2022.10.020.

[12] Z. Wei and J. Du. Reinforcement learning-based optimal trajectory tracking control of surface vessels under input saturations. *International Journal of Robust and Nonlinear Control*, 33(6): 3807–3825, 2023. doi: 10.1002/rnc.6597.

[13] J. Ning, Y. Ma, T. Li, C.L.Philip Chen, and S. Tong. Event-triggered based trajectory tracking control of under-actuated unmanned surface vehicle with state and input quantization. *IEEE Transactions on Intelligent Vehicles*, 9(2):3127–3139, 2024. doi: 10.1109/TIV.2023.3339852.

[14] G.C. Feng, P.W. Hao, H.N. Guo, and J.W. Li. Event-triggered simultaneous tracking control and stabilization of underactuated USVs. *Ocean Engineering*, 302:117680, 2024. doi: 10.1016/j.oceaneng.2024.117680.

[15] X. Hu, X. Gao, T. Li, and Y. Long. Dynamic event-triggered prescribed performance disturbance rejection fault-tolerant trajectory tracking for surface vehicles. *Ocean Engineering*, 312(1): 119063, 2024. doi: 10.1016/j.oceaneng.2024.119063.

[16] Y. Liu, Y. Sun, and L.Y. Hao. Nonsingular finite-time heading tracking control of marine vehicles with tracking error constraints. *Journal of the Franklin Institute*, 361(6):106734, 2024. doi: 10.1016/j.jfranklin.2024.106734.

[17] S. Song, Z. Liu, S. Yuan, Z. Wang, and T. Wang. A finite-time path following scheme of unmanned surface vessels with an optimization strategy. *ISA Transactions*, 146:61–74, 2024. doi: 10.1016/j.isatra.2024.01.016.

[18] H. Chen, H. Ren, Z. Gao, F. Yu, W. Guan, and D. Wang. Disturbance observer-based finite-time control scheme for dynamic positioning of ships subject to thruster faults. *International Journal of Robust and Nonlinear Control*, 31(13):6255–6271, 2021. doi: 10.1002/rnc.5610.

[19] N. Wang and Z. Deng. Finite-time fault estimator based fault-tolerance control for a surface vehicle with input saturations. *IEEE Transactions on Industrial Informatics*, 16(2):1172–1181, 2020. doi: 10.1109/TII.2019.2930471.

[20] N. Wang, H.R. Karimi, H. Li, and S.F. Su. Accurate trajectory tracking of disturbed surface vehicles: A finite-time control approach. *IEEE/ASME Transactions on Mechatronics*, 24(3): 1064–1074, 2019. doi: 10.1109/TMECH.2019.2906395.

[21] D. Zeng, C. Cai, J. Zhao, and Y. Liu. Practical fixed-time output feedback trajectory tracking control for marine surface vessels with unknown disturbances. *Control Engineering Practice*, 143:105789, 2024. doi: 10.1016/j.conengprac.2023.105789.

[22] P. Luo, D. Wu, A.S. Yamashita, N. Feng, and Y. Yang. Observer-based fixed-time dynamic surface tracking control for autonomous surface vehicles under actuator constraints and denial-of-service attacks. *Applied Mathematics and Computation*, 465:128403, 2024. doi: 10.1016/j.amc.2023.128403.

[23] Q. Guo, X. Zhang, and D. Ma. Adaptive fixed-time path following cooperative control for autonomous surface vehicles based on path-dependent constraints. *Applied Ocean Research*, 142:103826, 2024. doi: 10.1016/j.apor.2023.103826.

[24] J. Zhang, S. Yu, Y. Yan, and Y. Zhao. Fixed-time sliding mode trajectory tracking control for marine surface vessels under mismatched conditions and input saturation. *International Journal of Robust and Nonlinear Control*, 34(9):6142–6164, 2024. doi: 10.1002/rnc.7312.

[25] S. Souissi and M. Boukattaya. Time-varying nonsingular terminal sliding mode control of autonomous surface vehicle with predefined convergence time. *Ocean Engineering*, 263: 112264, 2022. doi: 10.1016/j.oceaneng.2022.112264.

[26] Z. Guo, J. Zhang, Y. Shang, Y. Zhang, L. Zhang, and W. Chen. Predefined-time global recursive sliding mode control for trajectory tracking of unmanned surface vehicles with disturbances uncertainties. *Ocean Engineering*, 313(2):119408, 2024. doi: 10.1016/j.oceaneng.2024.119408.

[27] H. Liu, X. Zhou, X. Tian, Q. Mai, and N. Sun. Predefined-time prescribed performance second-order sliding mode path following control for underactuated marine surface vehicles using self-structuring NN. *Ocean Engineering*, 309(1):118333, 2024. doi: 10.1016/j.oceaneng.2024.118333.

[28] G.X. Wu, Y. Ding, T. Tahsin, and I. Atilla. Adaptive neural network and extended state observer-based non-singular terminal sliding mode tracking control for an underactuated USV with unknown uncertainties. *Applied Ocean Research*, 135:103560, 2023. doi: 10.1016/j.apor.2023.103560.

[29] P. Herman. Robust trajectory tracking control scheme using transformed velocities for asymmetric underactuated marine vehicles. *Ocean Engineering*, 285(2):115379, 2023. doi: 10.1016/j.oceaneng.2023.115379.

[30] O. Elhaki and K. Shojaei. Robust saturated dynamic surface controller design for underactuated fast surface vessels including actuator dynamics. *Ocean Engineering*, 229:108987, 2021. doi: 10.1016/j.oceaneng.2021.108987.

[31] C. Zhang, C. Wang, J. Wang, and C. Li. Neuro-adaptive trajectory tracking control of underactuated autonomous surface vehicles with high-gain observer. *Applied Ocean Research*, 97: 102051, 2020. doi: 10.1016/j.apor.2020.102051.

[32] C. Zhang, C. Wang, Y. Wei, and J. Wang. Observer-based adaptive tracking control of underactuated autonomous marine vehicle with uncertainty dynamic. *Applied Ocean Research*, 101: 102364, 2020. doi: 10.1016/j.apor.2020.102364.

[33] C.Z. Pan, X.Z. Lai, S.X. Yang, and M. Wu. An efficient neural network approach to tracking control of an autonomous surface vehicle with unknown dynamics. *Expert Systems with Applications*, 40(5):1629–1635, 2013. doi: 10.1016/j.eswa.2012.09.008.

[34] C.Z. Pan, X.Z. Lai, S.X. Yang, and M. Wu. A biologically inspired approach to tracking control of underactuated surface vessels subject to unknown dynamics. *Expert Systems with Applications*, 42(4):2153–2161, 2015. doi: 10.1016/j.eswa.2014.09.042.

[35] G. Zhu and J. Du. Global robust adaptive trajectory tracking control for surface ships under input saturation. *IEEE Journal of Oceanic Engineering*, 45(2):442–450, 2020. doi: 10.1109/JOE.2018.2877895.

[36] C. Wu, G. Zhu, Y. Liu, and F. Li. Self-triggered adaptive neural control for usvs with sensor measurement sensitivity under deception attacks. *Journal of Field Robotics*, 42(1):153–168, 2024. doi: 10.1002/rob.22400.

[37] B. Huang, H. Peng, C. Zhang, and C.K. Ahn. Distributed optimal coordinated control for unmanned surface vehicles with interleaved periodic event-based mechanism. *IEEE Transactions on Vehicular Technology*, 73(12):18073–18086, 2024. doi: 10.1109/TVT.2024.3432736.

[38] B. Huang, X. Ren, B. Zhou, Z. Zhang, X. Zhou, and J. Miao. An intermittent anti-competition communication mechanism based formation maneuvers for the internet of unmanned surface vehicles. *IEEE Internet of Things Journal*, 2024. doi: 10.1109/JIOT.2024.3478784.

[39] H. Liu, J. Sun, J. Nie, and L. Zou. Observer-based adaptive second-order non-singular fast terminal sliding mode controller for robotic manipulators. *Asian Journal of Control*, 23(4): 1845–1854, 2021. doi: 10.1002/asjc.2369.

[40] S. Yi and J. Zhai. Adaptive second-order fast nonsingular terminal sliding mode control for robotic manipulators. *ISA Transactions*, 90:41–51, 2019. doi: 10.1016/j.isatra.2018.12.046.

[41] S. Mondal and C. Mahanta. Adaptive second order terminal sliding mode controller for robotic manipulators. *Journal of the Franklin Institute*, 351(4):2356–2377, 2014. doi: 10.1016/j.jfranklin.2013.08.027.

[42] T.I. Fossen and J.P. Strand. Passive nonlinear observer design for ships using Lyapunov methods: full-scale experiments with a supply vessel. *Automatica*, 35(1):3–16, 1999. doi: 10.1016/S0005-1098(98)00121-6.

[43] A. Li, Z. Shen, H. Bi, and H. Yu. Barrier Lyapunov function-based dual event-triggered prescribed performance path following control for marine surface vessel under input saturation. *Journal of the Franklin Institute*, 361(1):374–397, 2024. doi: 10.1016/j.jfranklin.2023.12.002.